

Slot opening displacement technique for cogging torque reduction of axial flux brushless DC motor for electric two-wheeler application

Introduction. Reduction of cogging torque is the crucial design consideration of axial flux brushless DC (BLDC) motor, particularly for low-speed applications. **Aim.** The slot opening displacement technique is presented in this article to reduce cogging torque in axial flux BLDC motors suitable for electric two-wheeler applications. **Methods.** Double rotor single stator configuration of axial flux BLDC motor is the most suitable for such vehicular applications. Initially double rotor single stator 250 W, 150 rpm axial flux BLDC motor is designed with stator slot opening in middle position and considered as reference motor for further analysis. To evaluate the cogging torque profile of the reference motor 3D finite element modeling and analysis are performed. The design is enhanced by dividing all stator teeth into groups and displacing the slot openings of each group in opposite direction with respect to the adjacent group. **Results.** The influence of slot opening displacement on cogging torque is evaluated with finite element modeling and analysis. As cogging torque is reduced from 1.23 N·m to 0.63 N·m, the slot opening displacement technique is found to be effective in reducing cogging torque of axial flux BLDC motor. References 26, table 2, figures 13.

Key words: axial flux brushless DC motor, cogging torque, slot opening displacement, design improvement, finite element analysis.

Вступ. Зменшення зубчастого обертаючого моменту є важливим фактором при проектуванні безщіткових двигунів постійного струму (БЩДПС) з осьовим потоком, особливо для низькошвидкісних застосувань. **Мета.** У цій статті представлений метод зміщення отвору щілини для зменшення зубчастого моменту в БЩДПС з осьовим потоком, придатних для застосування в електричних двоколісних транспортних засобах. **Методи.** Конфігурація двигуна постійного струму з осьовим потоком з двома роторами та одним статором є найбільш підходящою для таких транспортних засобів. Початково спроектований двороторний двигун БЩДПС з одним статором потужністю 250 Вт, 150 об/хв з осьовим потоком з отвором в статорному пазу в середньому положенні вважається еталонним двигуном для подальшого аналізу. Для оцінки профілю зубчастого обертаючого моменту еталонного двигуна виконується 3D-моделювання та аналіз методом скінченних елементів. Конструкція вдосконалена за рахунок поділу всіх зубів статора на групи та усунення пазових отворів кожної групи у протилежному напрямку по відношенню до сусідньої групи. **Результати.** Вплив зміщення отвору паза на зубчастий обертаючий момент оцінюється за допомогою моделювання та аналізу методом скінченних елементів. Оскільки зубчастий обертаючий момент зменшується з 1,23 Н·м до 0,63 Н·м, метод зміщення відкриття щілини виявився ефективним для зниження зубчастого обертаючого моменту двигуна БЩДПС з осьовим потоком. Бібл. 26, табл. 2, рис. 13.

Ключові слова: безщітковий двигун постійного струму з осьовим потоком, зубчастий обертаючий момент, зміщення отвору паза, удосконалення конструкції, аналіз методом скінченних елементів.

Introduction. Permanent magnet (PM) brushless motors are extensively used in various applications as it has attractive features like high efficiency, compactness, wide speed range, and fast dynamic response. The development in high energy PM materials and semiconductor switching devices has been the key factor in volume applications of PM brushless motors [1, 2]. PM brushless motors are generally categorized according to magnetic flux path as permanent radial flux magnet motors and permanent axial flux magnet motors [3]. The magnetic flux sets in radial direction and exciting current flows in axial direction in radial flux PM motors while magnetic flux sets in axial direction and exciting current flows in radial direction in axial flux PM motors. The better performance of axial flux PM motors over radial flux PM motors has attracted a lot of attention. Axial flux PM motors offer superior performance in terms of high efficiency, high power density, better utilization of copper, adjustable air-gap, and flat shape [4]. Due to these noteworthy merits axial flux PM motors are popularly used in typical applications like electric vehicles, elevators, robotics, servo drives, aerospace equipments, torpedo, and etc. [5]. In torque quality sensitive applications, torque ripple is one of the most significant performance characteristics. Vibration and noise are exacerbated by high torque ripple. It is important to note that the effects of high torque ripple are more objectionable in low speed range. Performance enhancement with torque ripple reduction of axial flux PM motors is highly indispensable particularly in low speed applications like electric vehicles.

Cogging torque and commutating torque due to distorted current and back electromotive force (EMF) waveforms are two components of torque ripple. The former is derived from variation of field energy due to slot reluctance variation and the later is derived due to harmonics in current and back EMF [6]. Cogging torque has greater effect on vibration, noise and start up performance. PM motors have inherent cogging torque due to the presence of PMs and a slotted stator structure. Because of the interaction between slot reluctance variation and the magneto motive force of PMs, cogging torque is inevitable. To improve the overall performance of axial flux brushless DC (BLDC) motors, it is critical to reduce cogging torque. Cogging torque can be lowered through PM motor design changes, whereas commutation torque can be reduced through control technique changes. It is always preferable to reduce cogging torque with design improvement since any reform in control technique will lead to compromise in efficiency. As a result, the focus of this research is on cogging torque reduction in axial flux BLDC motors through design reform.

Several techniques have been introduced to reduce cogging torque of radial flux PM motors like skewing of stator slots, skewing of magnets, dual skewing, displacement of pole, shaping of magnet pole, shaping and/or notching of stator tooth, notching of magnets, variation of pole arc, stepped slot opening shift, and etc. [7-16]. Genetic algorithms based optimization is done by changing the rotor design in terms of the magnet thickness, pole span and shape of the magnets for cogging

torque reduction of permanent magnet synchronous motor [17]. Among them only few techniques are directly applicable to axial flux permanent motors. Implementation cost and manufacturability are important factors that decide the applicability of design reforms for cogging torque reduction of PM axial flux motors. In radial flux PM motors, skewing the stator slot is more practicable than in axial flux PM motors. With the twin notched design of a radial flux surface mounted PM motor, cogging torque is minimized by using less PM material [18]. An effective technique for cogging torque reduction in axial flux PM motors is magnet skewing [19]. It is important to note that axial thrust increases along with reduction in cogging torque due to magnet skewing [20]. Variation of magnet pole arc reduces cogging torque with compromise in average torque and quality of back EMF waveform. Dual skew magnet technique is better option for cogging torque reduction of yoke less and segmented armature (YASA) axial flux PM motors [21]. Slot opening variation reduced cogging torque by 52 % of flat shape axial flux PM motor with main dimensions of 180 mm and 27 mm [22]. PMs with a relative displacement reduce cogging torque. As magnets are moved from a symmetrical to an unsymmetrical position, flux leakage increases [5]. In comparison to sector magnets and cylindrical magnets, sinusoidally shaped magnets perform better. With stator side adjustments such as slot opening shape variation and skewed slot opening, the cogging torque of an axial flux machine can be lowered [23]. Cogging torque of axial flux BLDC motor can be reduced with magnet notching technique. Magnet notching results in to increased unit cost of PM pole and reduced mechanical strength particularly when thickness of magnet is less [24].

This work focuses on reducing the cogging torque of axial flux brushless motor, as it is an important factor to be considered during design. The techniques pertaining to cogging torque reduction of radial flux PM motors are not directly applicable to axial flux PM motors in majority. Manufacturability and cost of implementation govern the real applicability of these techniques. Manufacturable and low-cost techniques are highly desirable in this context. Skewing of rotor and/or stator is effective method for cogging torque reduction of axial flux PM motors. However, axial force generation and manufacturing difficulties are the limitations of stator skewing of axial flux PM motors. In order to preclude abovementioned limitations, this paper proposes the slot opening displacement technique for cogging torque reduction of axial flux BLDC motors. There is no deterioration of back EMF waveform with displacement of slot as center lines of slots remain unchanged in the proposed technique. This technique is practically implementable and does not incur any extra cost.

Cogging torque. Cogging torque is caused by interaction of PMs and stator teeth hence it is the inherent characteristic of PM motors. PMs are the source of magnetic flux and stator teeth are source of reluctance variation. Air-gap reluctance variation is periodic hence cogging torque is also periodic in nature. Cogging torque is present even if stator winding is unexcited hence it is also named as no current torque. Equation (1) expresses the cogging torque in fundamental form [25]:

$$T_{cog}(\phi_{pm}, \theta_r) = -\frac{1}{2} \phi_{pm}^2 \frac{dR}{d\theta_r}, \quad (1)$$

where ϕ_{pm} , R , θ_r are the air-gap flux, air-gap reluctance and rotor angle, respectively.

Due to the periodicity cogging torque may be represented by Fourier series. Summation of interaction of each edge of PM with slot opening is the cogging torque. Following equation expresses the cogging torque produced without skewing in BLDC motors. Saturation and magnetic leakage are assumed to be negligible:

$$T_{cog} = \sum_{k=1}^{\infty} T_{N_p k} \sin(N_p k \alpha), \quad (2)$$

where k is the order of harmonics; N_p is the number of cycles of cogging torque in a rotor revolution. It is given by least common multiplier of number of slots N_s , and number of poles p ; α is the relative displacement between stator teeth and rotor; $T_{N_p k}$ is the coefficient produced due to Fast Fourier Transform (FFT) of the profile.

Above mentioned equation (2) is applied to each teeth obtain cogging torque. The total cogging torque is the sum of cogging torque caused by every stator teeth. $N_p k$ in (2) must be integer times pole numbers p . Expressing ratio of $N_p k$ to p as i , for an arbitrary teeth given by, its cogging torque becomes:

$$T_{scj} = \sum_{i=1}^{\infty} T_{sci} \sin pi(\alpha + \phi_j), \quad (3)$$

where T_{sci} is the Fourier coefficient; ϕ_j is the relative placement of the teeth j with reference teeth (teeth no. 1).

Hence, as per (3), total cogging torque can be calculated by adding all cogging torque components of all the N_s stator teeth:

$$T_{cog} = \sum_{j=1}^{N_s} \sum_{i=1}^{\infty} T_{sci} \sin pi \left(\alpha + \frac{2\pi}{N_s} (j-1) \right). \quad (4)$$

From (4), when p/N_s is an integer number, then irrespective of teeth number j ,

$$\sin pi \left(\alpha + \frac{2\pi}{N_s} (j-1) \right) = \sin pi \alpha. \quad \text{This shows that}$$

individual cogging torque developed by every stator teeth and the total cogging torque are cophasel. Hence, total cogging torque becomes N_s times the individual cogging torque and can be expressed as

$$T_{cog} = N_s \sum_{i=1}^{\infty} T_{sci} \sin pi \alpha, \quad (5)$$

cogging torque caused by different teeth is not in phase if p/N_s is not an integer. Then, it is difficult to simplify (4). Formation of a group of certain number of adjacent slots is required for solution. The groups are chosen on the basis that the cogging torque developed by various groups is cophasel. Therefore, the total cogging torque may be explicitly linked with the cogging torque of individual group directly.

Take λ adjacent slots (teeth) as one group then $\lambda = N_p/p$. From this, the number of groups will be n , where $n = N_s p / N_p$. For a certain teeth j , the cogging torque is given by (3). Equation (3) can be rewritten as

$$T_{scgj} = \sum_{i=1}^{\infty} T_{sci} \sin pi \left(\alpha + \frac{2\pi}{N_s} (j-1) \right). \quad (6)$$

The cogging torque generated by a particular group having λ teeth is the summation of the cogging torques developed by each teeth of this group and is given by:

$$T_{cog_g} = \sum_{j=1}^{\lambda} \sum_{i=1}^{\infty} T_{sci} \sin \left[pi \left(\alpha + \frac{2\pi}{N_s} (j-1) \right) \right]. \quad (7)$$

The simplification of (6) is as:

$$T_{cog_g} = \sum_{i=1}^{\infty} T_{sci} \frac{\sin \frac{p\lambda\pi i}{N_s}}{\sin \frac{p\pi i}{N_s}} \sin \left(pi\alpha + \frac{p\lambda\pi i}{N_s} - \frac{p\pi i}{N_s} \right). \quad (8)$$

As $p\lambda i/N_s$ in (8) is an integer number the $\sin(p\lambda\pi i/N_s)$ is 0. Hence, for certain harmonic index i only the cogging torque component will exist. Equation (8) can be simplified to these i values as

$$T_{cog_g} = \sum_{i=1}^{\infty} T_{sci} \lambda \sin pi\alpha. \quad (9)$$

Total cogging torque can be calculated by multiplying the cogging torque of single group given by (9) with number of groups (n) as:

$$T_{cog} = n \sum_{i=1}^{\infty} T_{sci} \lambda \sin pi\alpha. \quad (10)$$

Axial flux BLDC motor. 3D view of double rotor single stator axial flux motor considered in present work is shown in Fig. 1. Motor rating of 250 W, 150 rpm determined for electric two-wheeler application based on application needs and system dynamics. Application requirements include a laden vehicle weight of 150 kg, top speed of 25 km/h and acceleration of 0-25 km/h in 9 s.

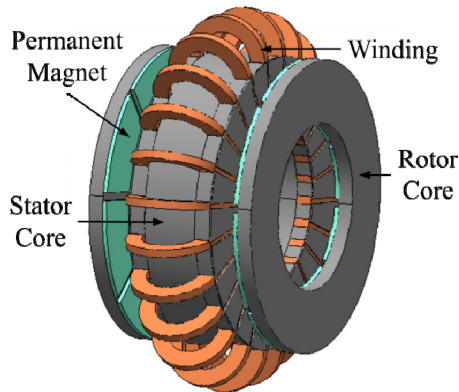


Fig. 1. Axial flux BLDC motor

Axial flux dual rotor single stator BLDC motor is designed with 48 stator slots and 16 rotor poles. Stator core is made of siliceous material of high relative permeability and laminated in order to reduce eddy current losses. Stator consists back to back ring type winding. Back-to-back ring type winding results in to short over hang. Rotor comprises rotor core and surface mount PMs. Rotor core is made of high relative permeability soft iron material. High energy NdFeB grade 50 type PM material is selected to obtain high power density and better overall performance of motor.

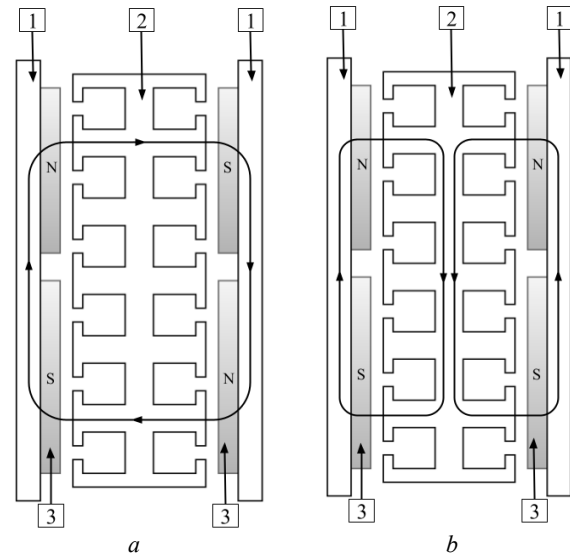
Design of motor is carried out based on various design variables like magnetic and electric loadings, current density, conductor packing factor, diametric ratio, number of slots/pole/phase, magnet fraction, permissible flux density in core section, and etc. Diametric ratio is

assumed to be $\sqrt{3}$ to obtain optimum power density [26]. None of the cogging torque reduction technique is applied to the initially designed motor. Initially designed motor has slot openings in middle of slot and all stator teeth are symmetrically placed over the stator periphery. Initially designed motor is considered to be the reference motor for further analysis and performance comparison. Table 1 displays the important design parameters of reference motor.

Table 1
Design parameters of reference motor

Motor parameters	Value
Outer diameter, D_o	182 mm
Inner diameter, D_i	104 mm
Number of slots, N_s	48
Number of pole pair, p	16
Magnet length, L_m	2.7 mm
Length of air-gap, L_g	0.5 mm
Type of PM	NdFeB, Grade 50
PM remanence, B_r	1.2 T
Core material type	M19

According to the polarity of opposite PMs, a double rotor sandwiched stator axial flux motor can be classified as NN or NS. In a NN type motor, two opposite magnets have the same polarity, whereas two opposite magnets have opposite polarities in NS topology as shown in Fig. 2,a,b respectively.



1 – rotor core; 2 – stator core; 3 – PM

Fig. 2. Flux path: (a) – NN topology; (b) – NS topology

This research work is focused on NN type axial flux PM motor. As shown in Fig. 2,a magnetic flux emanates from a PM, traverses the air-gap, travels through the stator core, and closes the circuit to the opposite polarity PM. Axial flux PM motors consist a disc type motor stator having a roll stacked structure including teeth, slots, and a back iron section. The tooth and the slot are formed to be apart from each other on both sides of a spiral wound ring-shaped laminated core along a circumference direction and the windings are inserted into the slots. Slots are created on spiral wound core with CNC laser cutting machines as per design calculation.

Figure 3 shows a rotor disc with 8 poles of PM material of the NdFeB type and Fig. 4 shows stator core of initially designed reference motor with slot openings in middle position and its close up view.

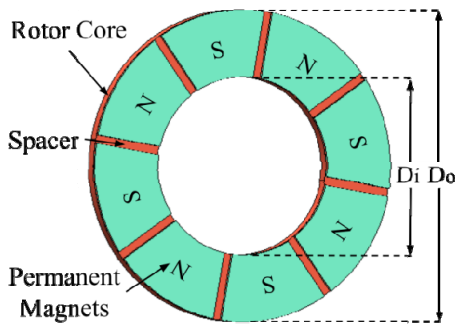


Fig. 3. Rotor disc of reference motor

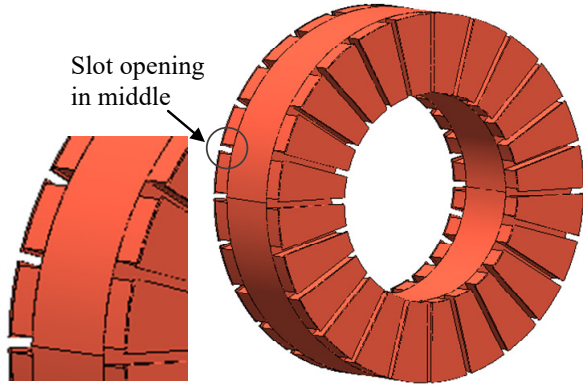


Fig. 4. Stator core of reference motor

3D modelling and simulation is required for accurate electromagnetic analysis of axial flux BLDC motor. 3D Finite Element Analysis (FEA) gives precise results considering geometric details and magnetic non-linearity. Complexity in modelling and considerable time for simulation are limitations of 3D modelling and simulation. Modelling and simulation is carried out with finite element software MagNet7.1 that is commercially available. According to the design outcome, a 3D model is created and appropriate materials are assigned. Tetrahedral elements are used to form the mesh, and boundary constraints are assigned. At different rotor position cogging torque is obtained with FEA. This technique is repeated until the final rotor position is obtained through incremental rotor position.

The cogging torque profile is plotted using the results of the cogging torque at different rotor positions. Variation of cogging torque with respect to rotor position is periodic in nature because of symmetrical structure of motor. Figure 5 illustrates the flow chart for the exercise to obtain cogging torque profile.

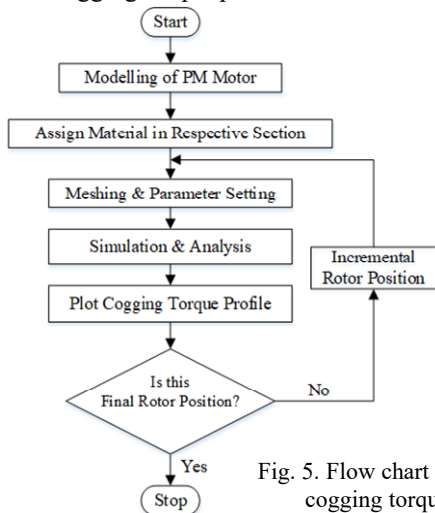


Fig. 5. Flow chart to obtain cogging torque profile

It is analysed that reference axial flux BLDC motor has 2.46 N·m peak to peak cogging torque as illustrated in Fig. 6.

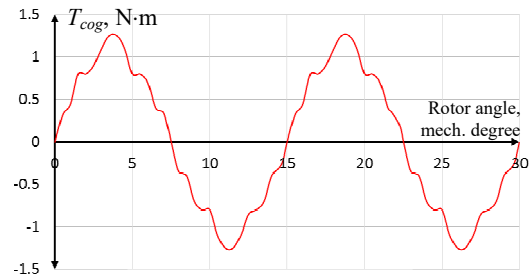


Fig. 6. Cogging torque profile of initially designed motor

Slot displacement technique. Various design strategies for cogging torque reduction of radial flux brushless motors can be found in archival literature. This section discusses techniques of axial flux BLDC motors' cogging torque reduction. Undesirable axial force is generated due to skewing of stator and/or rotor. The quality of back EMF gets deteriorated in conventional skewing because of decentralizing in winding function. Variation of pole arc adversely affect quality of back EMF waveform and average torque. Because of the interaction between air-gap flux and air-gap reluctance variation, cogging torque is produced in axial flux BLDC motors. By reducing air-gap reluctance variation, cogging torque can be reduced. This section presents modified structure based on displacement of stator slot openings. As there is no skewing or pole arc variation, the related demerits of those techniques are removed. Other performance parameters of proposed topology are in line with skewed motor. The displacement of slot openings results in smoothing air-gap reluctance variation. Because the slot openings are the main source of air-gap reluctance variation, it is important to displace only slot openings so as to obtain trapezoidal back EMF and less cogging torque. It is important to note that only slot openings are displaced keeping slot center lines fixed. Stator slots are grouped and slot openings are displaced in anti-clockwise and clockwise respectively in group as illustrated in Fig. 7, b. Figure 7, a represents reference design.

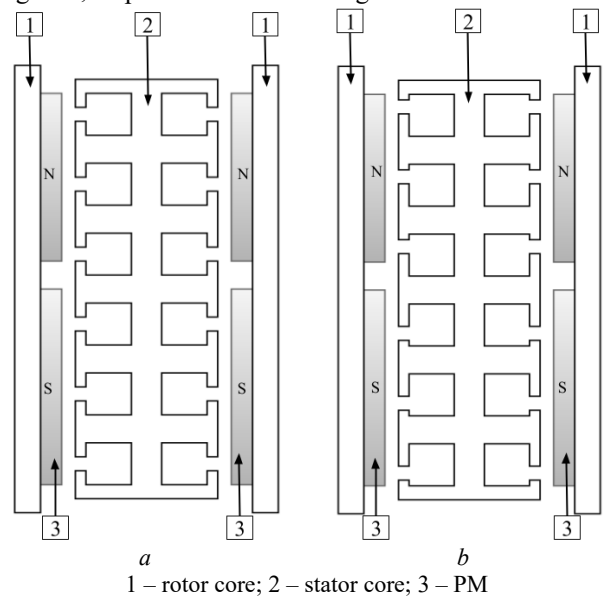


Fig. 7. (a) – reference design of slot; (b) – improved slots with displaced openings

Figures 8, a, b illustrate modified stator core and its close up view with slot openings displaced by 0.75° in anti-

clockwise and clockwise respectively in group. It is important to note that only slot openings have been displaced keeping all other dimensions i.e. stator outer diameter, stator inner diameter, slot area, slot width, slot depth, and etc. same as initially designed reference motor.

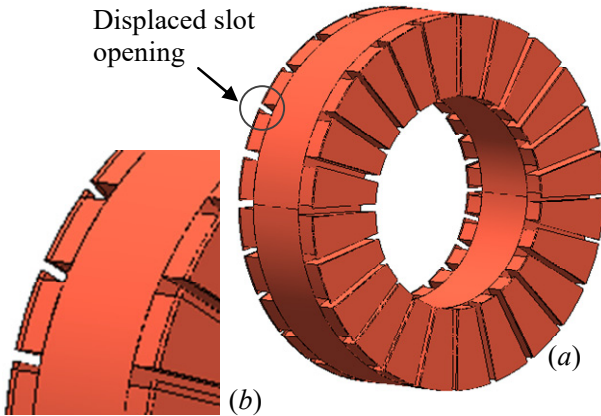


Fig. 8. (a) – improved stator core with shifted slot openings; (b) – improved stator core with shifted slot openings

Simulation and results. The slot opening displacement technique described in previous section is applied to reference axial flux PM motor having design details as per Table 1. The motor considered in present work has total 48 stator slots and number of slots on each side of rotor are 24. Each stator side has 8 groups of slots having 3 slots in each group. Slot openings of one group are displaced in clockwise direction while slot openings of adjacent group are displaced in anti-clockwise direction. Cogging torque developed by each group can be determined from (10). Due to displacement of stator slot openings in opposite direction, the cogging torque developed by adjacent group is not co-phasal hence combined cogging torque of two groups is reduced which leads to reduction of overall cogging torque. Axial flux permanent BLDC motors possess non-linear characteristic in addition to the leakage flux, fringing, manufacturing tolerances, and etc. Since FEA offer accurate and realistic results considering above-mentioned typical motor characteristics, to present effectiveness of proposed slot opening displacement technique 3D FEA has been performed. Cogging torque profile of reference motor and improved motor are displayed in Fig. 9.

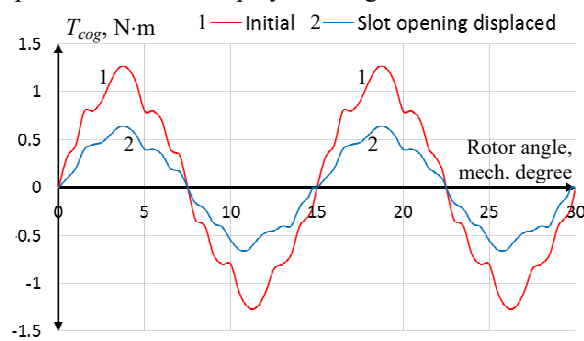


Fig. 9. Comparison between cogging torque profiles

As mentioned in Table 2 the reference axial flux BLDC motor has peak to peak cogging torque of 2.46 N·m. while improved motor with slot opening displacement has peak to peak cogging torque of 1.26 N·m. Peak to peak cogging torque is reduced from 2.46 N·m to 1.26 N·m with marginal compromise in average torque.

Table 2

Comparison of the reference and upgraded axial flux motor designs

Sr. no.	Parameters	Initial	Upgraded design with slot opening shift
1	Cogging torque, N·m	2.46	1.26
2	Average torque, N·m	15.85	14.65

The FFT analysis of the profile of cogging torque is shown in Fig. 10. Cogging torque fundamental and even order components are reduced significantly, as indicated.

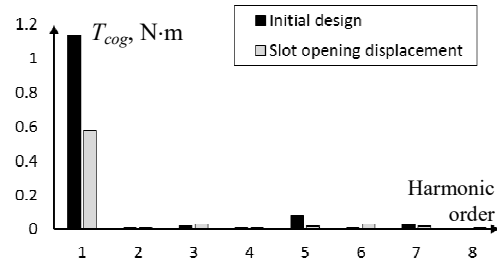


Fig. 10. FFT analysis of cogging torque profile

It's necessary to compare the back EMF waveforms of the reference and upgraded motors [26]. Comparison of back EMF waveforms before and after application of slot displacement technique is depicted in Fig. 11. Back EMF waveform is improved with slot opening displacement technique in comparison to the initially designed reference motor.

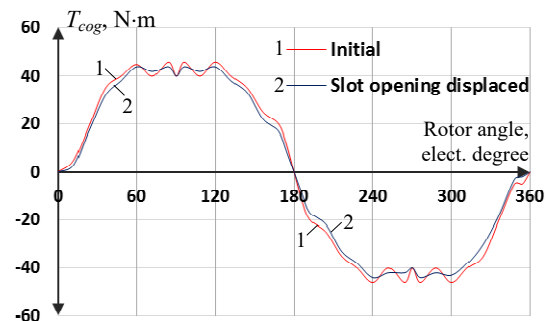


Fig. 11. Back EMF wave forms of reference design and improved design

The FFT analysis of back EMF profile is shown on Fig. 12. It is observed that fundamental component is slightly reduced from 48 V to 45.9 V and total harmonic distortion is reduced from 13.73 % to 12.41 %.

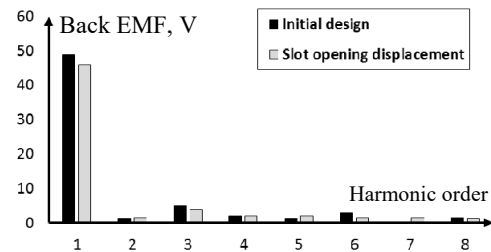


Fig. 12. FFT analysis of back EMF waveforms

Electromagnetic field analysis is performed to evaluate flux densities in various motor sections and to validate reference and improved designs. Maxwell's equations are fundamental equations governing interaction of electric and magnetic fields within an electrical machine.

Finite element method is used to solve this equation for flux density calculation. Assessing the flux density in

different motor parts is very important because it is one of the key design variables. Iron losses and overall performance of motor are influenced by flux density. Flux density is assumed based on expected performance and properties of magnetic material. If actual flux density surpasses maximum permissible flux density of respective material, motor operates in the region of saturation with reduced efficiency. Opposite to that if actual flux density is below the assumed flux density than derating of motor and poor utilization of material is observed.

Figure 13 shows flux density distribution in improved stator with displaced slot openings. It is examined that there is close agreement between actual flux densities and assumed flux densities in various sections. Analytical design of magnetic sections is validated on account of closeness between assumed and real flux densities.

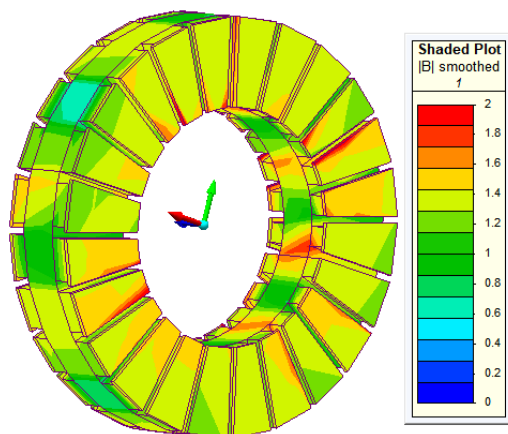


Fig. 13. Flux density plot of improved stator

Conclusion. Reduction of the cogging torque of axial flux brushless DC motors designed for low speed vehicular applications is highly desirable. This paper presents slot opening displacement technique for cogging torque reduction of double rotor sandwiched stator surface permanent magnet axial flux brushless DC motor. The motor that was initially designed is used as a reference motor, and its electromagnetic analysis is done using 3D finite element analysis. Slot opening displacement is performed to 48 slot 16 pole double rotor sandwiched stator axial flux brushless DC motor with an objective of cogging torque reduction. It is analysed that peak to peak cogging torque is reduced by 48.78 % with marginal reduction in average torque. Back electromotive force wave form of improved motor remains symmetrical. Slot opening displacement technique is effective in reduction of cogging torque of double rotor sandwiched stator axial flux brushless DC motor and can be applied to other topologies of permanent magnet motors as well.

Conflict of interest. The author declares no conflict of interest.

REFERENCES

1. Akkouchi K., Rahmani L., Lebied R. New application of artificial neural network-based direct power control for permanent magnet synchronous generator. *Electrical Engineering & Electromechanics*, 2021, no. 6, pp. 18-24. doi: <https://doi.org/10.20998/2074-272X.2021.6.03>.
2. Panchal T.H., Patel A.N., Patel R.M. Reduction of cogging torque of radial flux permanent magnet brushless DC motor by magnet shifting technique. *Electrical Engineering &*

- Electromechanics*, 2022, no. 3, pp. 15-20. doi: <https://doi.org/10.20998/2074-272X.2022.3.03>
3. Chan C.C. Axial-Field Electrical Machines - Design and Applications. *IEEE Transactions on Energy Conversion*, 1987, vol. EC-2, no. 2, pp. 294-300. doi: <https://doi.org/10.1109/TEC.1987.4765844>.
4. Aydin M., Huang S., Lipo T. A. Axial Flux Permanent Magnet Disc Machines: A Review. *Research Report*, 2004, no. 10, pp. 1-11.
5. Rahim N.A., Ping H.W., Tadjuddin M. Design of Axial Flux Permanent Magnet Brushless DC Motor for Direct Drive of Electric Vehicle. *2007 IEEE Power Engineering Society General Meeting*, 2007, pp. 1-6. doi: <https://doi.org/10.1109/PES.2007.385615>.
6. Aydin M., Zhu Z.Q., Lipo T.A., Howe D. Minimization of Cogging Torque in Axial-Flux Permanent-Magnet Machines: Design Concepts. *IEEE Transactions on Magnetics*, 2007, vol. 43, no. 9, pp. 3614-3622. doi: <https://doi.org/10.1109/TMAG.2007.902818>.
7. Islam R., Husain I., Fardoun A., McLaughlin K. Permanent Magnet Synchronous Motor Magnet Designs with Skewing for Torque Ripple and Cogging Torque Reduction. *2007 IEEE Industry Applications Annual Meeting*, 2007, pp. 1552-1559. doi: <https://doi.org/10.1109/07IAS.2007.240>.
8. Chu W.Q., Zhu Z.Q. Investigation of Torque Ripples in Permanent Magnet Synchronous Machines With Skewing. *IEEE Transactions on Magnetics*, 2013, vol. 49, no. 3, pp. 1211-1220. doi: <https://doi.org/10.1109/TMAG.2012.2225069>.
9. Chabchoub M., Ben Salah I., Krebs G., Neji R., Marchand C. PMSM cogging torque reduction: Comparison between different shapes of magnet. *2012 First International Conference on Renewable Energies and Vehicular Technology*, 2012, pp. 206-211. doi: <https://doi.org/10.1109/REVET.2012.6195272>.
10. Jong Gun Lee, Yu Ki Lee, Gwan Soo Park. Effects of V-skew on the cogging torque in permanent magnet synchronous motor. *2013 International Conference on Electrical Machines and Systems (ICEMS)*, 2013, pp. 122-124. doi: <https://doi.org/10.1109/ICEMS.2013.6754536>.
11. Boukais B., Zeroug H. Magnet Segmentation for Commutation Torque Ripple Reduction in a Brushless DC Motor Drive. *IEEE Transactions on Magnetics*, 2010, vol. 46, no. 11, pp. 3909-3919. doi: <https://doi.org/10.1109/TMAG.2010.2057439>.
12. Wenliang Zhao, Lipo T.A., Byung-II Kwon. Material-Efficient Permanent-Magnet Shape for Torque Pulsation Minimization in SPM Motors for Automotive Applications. *IEEE Transactions on Industrial Electronics*, 2014, vol. 61, no. 10, pp. 5779-5787. doi: <https://doi.org/10.1109/TIE.2014.2301758>.
13. Bin Zhang, Xiuhe Wang, Ran Zhang, Xiaolei Mou. Cogging torque reduction by combining teeth notching and rotor magnets skewing in PM BLDC with concentrated windings. *2008 International Conference on Electrical Machines and Systems*, 2008, pp. 3189-3192.
14. Petrov I., Ponomarev P., Alexandrova Y., Pyrhonen J. Unequal Teeth Widths for Torque Ripple Reduction in Permanent Magnet Synchronous Machines With Fractional-Slot Non-Overlapping Windings. *IEEE Transactions on Magnetics*, 2015, vol. 51, no. 2, pp. 1-9. doi: <https://doi.org/10.1109/TMAG.2014.2355178>.
15. Park G.-J., Kim Y.-J., Jung S.-Y. Design of IPMSM Applying V-Shape Skew Considering Axial Force Distribution and Performance Characteristics According to the Rotating Direction. *IEEE Transactions on Applied Superconductivity*, 2016, vol. 26, no. 4, pp. 1-5. doi: <https://doi.org/10.1109/TASC.2016.2543267>.
16. Upadhayay P., Rajagopal K.R. Torque ripple reduction using magnet pole shaping in a surface mounted Permanent Magnet BLDC motor. *2013 International Conference on Renewable Energy Research and Applications (ICRERA)*, 2013, pp. 516-521. doi: <https://doi.org/10.1109/ICRERA.2013.6749809>.
17. Sarac V. Performance optimization of permanent magnet synchronous motor by cogging torque reduction. *Journal of Electrical Engineering*, 2019, vol. 70, no. 3, pp. 218-226. doi: <https://doi.org/10.2478/jee-2019-0030>.

18. Yu H.-C., Yu B.-S., Yu J., Lin C.-K. A Dual Notched Design of Radial-Flux Permanent Magnet Motors with Low Cogging Torque and Rare Earth Material. *IEEE Transactions on Magnetics*, 2014, vol. 50, no. 11, pp. 1-4. doi: <https://doi.org/10.1109/TMAG.2014.2329139>.

19. Aydin M., Gulec M. Reduction of Cogging Torque in Double-Rotor Axial-Flux Permanent-Magnet Disk Motors: A Review of Cost-Effective Magnet-Skewing Techniques With Experimental Verification. *IEEE Transactions on Industrial Electronics*, 2014, vol. 61, no. 9, pp. 5025-5034. doi: <https://doi.org/10.1109/TIE.2013.2276777>.

20. Park G.-J., Kim Y.-J., Jung S.-Y. Design of IPMSM Applying V-Shape Skew Considering Axial Force Distribution and Performance Characteristics According to the Rotating Direction. *IEEE Transactions on Applied Superconductivity*, 2016, vol. 26, no. 4, pp. 1-5. doi: <https://doi.org/10.1109/TASC.2016.2543267>.

21. Jia L., Lin M., Le W., Li N., Kong Y. Dual-Skew Magnet for Cogging Torque Minimization of Axial Flux PMSM With Segmented Stator. *IEEE Transactions on Magnetics*, 2020, vol. 56, no. 2, pp. 1-6. doi: <https://doi.org/10.1109/TMAG.2019.2951704>.

22. Wanjiku J., Khan M.A., Barendse P.S., Pillay P. Influence of Slot Openings and Tooth Profile on Cogging Torque in Axial-Flux PM Machines. *IEEE Transactions on Industrial Electronics*, 2015, vol. 62, no. 12, pp. 7578-7589. doi: <https://doi.org/10.1109/TIE.2015.2458959>.

23. Kumar P., Srivastava R.K. Cost-Effective Stator Modification Techniques for Cogging Torque Reduction in Axial Flux Permanent

Magnet Machines. *2018 IEEE Transportation Electrification Conference and Expo, Asia-Pacific (ITEC Asia-Pacific)*, 2018, pp. 1-5. doi: <https://doi.org/10.1109/ITEC-AP.2018.8433291>.

24. Patel A.N., Suthar B.N. Cogging Torque Reduction of Sandwiched Stator Axial Flux Permanent Magnet Brushless DC Motor using Magnet Notching Technique. *International Journal of Engineering*, 2019, vol. 32, no. 7, pp. 940-946. doi: <https://doi.org/10.5829/ije.2019.32.07a.06>.

25. Dosiak L., Pillay P. Cogging Torque Reduction in Permanent Magnet Machines. *IEEE Transactions on Industry Applications*, 2007, vol. 43, no. 6, pp. 1565-1571. doi: <https://doi.org/10.1109/TIA.2007.908160>.

26. Surong Huang, Jian Luo, Leonardi F., Lipo T.A. A general approach to sizing and power density equations for comparison of electrical machines. *IEEE Transactions on Industry Applications*, 1998, vol. 34, no. 1, pp. 92-97. doi: <https://doi.org/10.1109/28.658727>.

Received 22.08.2022

Accepted 21.12.2022

Published 07.03.2023

A.N. Patel¹, PhD, Associate Professor,

¹ Department of Electrical Engineering,

Institute of Technology, Nirma University, India,

e-mail: amit.patel@nirmauni.ac.in (Corresponding Author)

How to cite this article:

Patel A.N. Slot opening displacement technique for cogging torque reduction of axial flux brushless DC motor for electric two-wheeler application. *Electrical Engineering & Electromechanics*, 2023, no. 2, pp. 7-13. doi: <https://doi.org/10.20998/2074-272X.2023.2.02>